

Gauge ambiguity of the quark spectrum in the Color Glass Condensate

François Gelis ^a, Naoto Tanji ^b

- a. Institut de Physique Théorique, Université Paris-Saclay
CEA, CNRS, F-91191 Gif-sur-Yvette, France
- b. European Centre for Theoretical Studies in Nuclear Physics
and Related Areas (ECT*) and Fondazione Bruno Kessler
Villa Tambosi, Strada delle Tabarelle 286, I-38123 Villazzano, Italy

Abstract

In the Color Glass Condensate, the inclusive spectrum of produced quarks in a heavy ion collision is obtained as the Fourier transform of a 2-fermion correlation function. Due to its non-locality, the two points of this function must be linked by a Wilson line in order to have a gauge invariant result, but when the quark spectrum is evaluated in a background that has a non-zero chromo-magnetic field, this procedure suffers from an ambiguity related to the choice of the contour defining the Wilson line. In this paper, we use an analytically tractable toy model of the background field in order to study this contour dependence. We show that for a straight contour, unphysical contributions to the spectrum in p_{\perp}^{-2} and p_{\perp}^{-3} cancel, leading to a spectrum with a tail in p_{\perp}^{-4} . If the contour defining the Wilson line deviates from a straight line, the path dependence is at most of order p_{\perp}^{-5} if its curvature is bounded, and of order p_{\perp}^{-4} otherwise. When the contour is forced to go through a fixed point, the path dependence is even larger, of order p_{\perp}^{-2} .

1 Introduction

High energy collisions between hadrons or nuclei probe the constituents of the projectiles that carry a very small fraction of the available longitudinal momentum. In

this kinematical domain, the gluon occupation number rises, and saturates at non-perturbatively large values of order of the inverse strong coupling, α_s^{-1} . The domain where exists such a large gluon occupation number is delimited by virtualities $Q^2 \leq Q_s^2(x)$, where $Q_s(x)$ is a momentum scale that depends on the longitudinal momentum fraction x (and therefore of the collision energy), called the *saturation momentum*.

In addition to controlling the onset of gluon saturation, the scale $Q_s(x)$ is also the typical transverse momentum of the saturated gluons. This means that it also controls whether multiple scattering corrections are important: a process whose characteristic transverse momentum scale is of order $Q_s(x)$ or smaller receives important corrections due to scatterings on multiple gluons. In particular, this plays an important role in the question of quark production. In this case, the characteristic momentum scale is the *transverse mass*, $M_p^2 \equiv (m^2 + p_\perp^2)^{1/2}$, that combines the transverse momentum of the produced quark and its mass. When $M_p \gg Q_s$, quark production is perturbative, i.e. dominated by the usual two-gluon process, $gg \rightarrow Q\bar{Q}$. In contrast, when $M_p \lesssim Q_s$, processes involving more than two incoming gluons are equally important. However, the usual framework of collinear factorization is not well suited to cope with these multi-gluon corrections, since in its standard form it provided only a handle on the single-gluon distribution inside a hadronic projectile. Instead, one can use the Color Glass Condensate (CGC) effective theory [1, 2, 3, 4, 5], in which a high energy projectile is described by a color current on the light-cone [6, 7]. At lowest order, the CGC description is purely classical, thanks to the large gluon occupation number.

In this framework, the collision of two hadrons or nuclei produces a color field of order $A^\mu \sim g^{-1}$, determined by solving the classical Yang-Mills equations [8, 9, 10] with a source made of the superposition of the color currents of the two projectiles (the boundary conditions should be retarded for inclusive observables) [11, 12]. Quark production can then be viewed as a problem of particle production in a time-dependent external field [13, 14, 15, 16, 17, 18, 19, 20, 21]. In particular, the inclusive quark spectrum can be expressed in terms of solutions of the Dirac equation in this external field. More precisely, one needs the *mode functions* of the Dirac equation, i.e. spinors whose initial condition is a remote past is a free spinor and that are evolved over the external field up to the time at which the quark spectrum is evaluated. The quark spectrum is then obtained as the spatial Fourier transform of an equal-time bilinear combination of these mode functions, $\psi^\dagger(t, \mathbf{x})\psi(t, \mathbf{y})$.

Note however that a non-local object such as $\psi^\dagger(t, \mathbf{x})\psi(t, \mathbf{y})$ is not gauge invariant. This can be remedied by inserting a Wilson line between the two spinors,

$$\psi^\dagger(t, \mathbf{x})\psi(t, \mathbf{y}) \rightarrow \psi^\dagger(t, \mathbf{x}) W_\gamma(\mathbf{x}, \mathbf{y}) \psi(t, \mathbf{y}),$$

defined on a contour γ that connects the points \mathbf{x} and \mathbf{y} . When the external color field at the time t where the quark spectrum is evaluated is null (in fact, any pure

gauge works for this argument), the Wilson line W_γ is independent of the path γ and the above modification suffers no ambiguity. But there are situations where the external field at the time t is not a pure gauge (this is the case in the CGC description of heavy ion collisions at a finite time after the collision). When this happens, the above definition –although gauge invariant– is ambiguous because it generally depends on the choice of the path γ . Note that this is not an issue in collisions between a dilute and a dense –saturated– projectile, since one may expand the yield in powers of the density of color charges in the dilute projectile. The final state dressing by a Wilson line would be of higher order in this density [22, 23, 24, 25].

In this paper, we construct a toy configuration of CGC color currents, using the $SU(2)$ group for additional simplicity, such that the classical color fields are simple enough to allow a semi-analytic discussion of the dependence of the quark spectrum on the path γ . Our paper is organized as follows. In the section 2, we describe the setup of the external field. Then, in the section 3, we recall the expression of the quark spectrum in terms of the fermionic mode functions and evaluate it at a proper time $\tau = 0^+$, i.e. just after the collision. We also discuss the pathologies of this spectrum when no Wilson line is included to make it gauge invariant. In the section 4, we study the effect of a Wilson line defined by a straight path between the points \mathbf{x} and \mathbf{y} . We explain how to perform the asymptotic expansion of the spectrum at large transverse momentum, and derive the leading term, in order to show that the pathologies encountered without a Wilson line have now been fixed. The section 5 discusses the differences that may arise when using a curved path to define the Wilson line. We use the non-Abelian Stokes theorem in order to relate the leading term of the asymptotic expansion of the quark spectrum to properties of the path γ , such as its curvature. Finally, summary and conclusions are in the section 6, and a few more technical results are relegated into three appendices.

2 Background field setup

In order to address these questions with a setup that allows an analytical treatment, we consider an $SU(2)$ gauge group with a very special configuration of color sources for the two projectiles, which was introduced in [26]. Let us first recall the link between these sources and the color field generated immediately after the collision. Starting from the color current carried by the two projectiles,

$$J_a^\mu(x) \equiv \delta^{\mu-} \delta(x^+) \rho_{1a}(\mathbf{x}_\perp) + \delta^{\mu+} \delta(x^-) \rho_{2a}(\mathbf{x}_\perp), \quad (1)$$

we first construct Wilson lines

$$U_m(\mathbf{x}_\perp) \equiv \exp \left(-ig \frac{1}{\nabla_\perp^2} \rho_m(\mathbf{x}_\perp) \right). \quad (2)$$

These Wilson lines enter in the expression of the (light-cone gauge) color field before the collision for each projectile,

$$\alpha_m^i(\mathbf{x}_\perp) = \frac{i}{g} U_m^\dagger(\mathbf{x}_\perp) \partial^i U_m(\mathbf{x}_\perp), \quad \alpha_m^\pm = 0. \quad (3)$$

The non-zero components (we work in the Fock-Schwinger gauge, in which $A^\tau = 0$) of the color field in the forward light-cone just after the collision (i.e. at a proper time $\tau = 0^+$) are then given by [11]

$$A^i(\tau = 0^+, \mathbf{x}_\perp) = \alpha_1^i(\mathbf{x}_\perp) + \alpha_2^i(\mathbf{x}_\perp), \quad A^\eta(\tau = 0^+, \mathbf{x}_\perp) = \frac{ig}{2} [\alpha_1^i(\mathbf{x}_\perp), \alpha_2^i(\mathbf{x}_\perp)]. \quad (4)$$

An analytically tractable setup consists in having homogeneous fields $\alpha_{1,2}^i$ before the collision, which can be achieved if the argument of the exponential in $U_{1,2}(\mathbf{x}_\perp)$ is linear,

$$U_m(\mathbf{x}_\perp) = \exp(i \mathbf{Q}_m \cdot \mathbf{x}_\perp \sigma^m). \quad (5)$$

To further simplify this setup, the Wilson line U_1 has been chosen to involve only the color generator σ^1 , and U_2 involves only σ^2 . The vectors $\mathbf{Q}_{1,2}$ are fixed transverse vectors having the dimension of a mass. With these Wilson lines, we have

$$\alpha_m^i = \frac{1}{g} Q_m^i \sigma^m, \quad (6)$$

and

$$A^i(\tau = 0^+) = \frac{1}{g} (Q_1^i \sigma^1 + Q_2^i \sigma^2), \quad A^\eta(\tau = 0^+) = -\frac{1}{g} (\mathbf{Q}_1 \cdot \mathbf{Q}_2) \sigma^3. \quad (7)$$

Since these fields are constant elements of the $SU(2)$ algebra, the evaluation of Wilson lines in such a background is considerably simplified.

In order to gain some further insight on the role played by the orientations of the vectors $\mathbf{Q}_{1,2}$, we can also calculate the chromo-electric and chromo-magnetic fields just after the collision,

$$\mathbf{E} = \frac{2}{g} (\mathbf{Q}_1 \cdot \mathbf{Q}_2) \hat{z} \sigma^3, \quad \mathbf{B} = \frac{2}{g} (\mathbf{Q}_1 \times \mathbf{Q}_2) \sigma^3. \quad (8)$$

Thus, we see that the radiated field is purely electric if \mathbf{Q}_1 and \mathbf{Q}_2 are parallel, and purely magnetic when they are orthogonal. Intermediate orientations lead to a mixture of electrical and magnetic fields.

3 Inclusive quark spectrum

In the collisions of two hadron/nuclei described by CGC, the inclusive spectrum of produced quarks can be expressed as follows [18],

$$\frac{dN}{dy_p d^2\mathbf{p}_\perp} = \frac{1}{8\pi(2\pi)^3 L_\eta} \sum_{s,s'} \sum_{a,a'} \int \frac{d^2\mathbf{k}_\perp}{(2\pi)^2} \frac{d\nu}{2\pi} \frac{d\nu'}{2\pi} \left| \left(\widehat{\psi}_{\mathbf{p}_\perp \nu' s' a'}^{0+} | \widehat{\psi}_{\mathbf{k}_\perp \nu s a}^- \right)_{\tau=0^+} \right|^2. \quad (9)$$

In this formula, $\widehat{\psi}_{\mathbf{p}_\perp \nu' s' a'}^{0+}$ is a free positive energy spinor of transverse momentum \mathbf{p}_\perp , rapidity ν' , spin s' and color a' . $\widehat{\psi}_{\mathbf{k}_\perp \nu s a}^-$ is a spinor that has interacted with the background color field, starting at $x^0 = -\infty$ as a negative energy spinor of transverse momentum \mathbf{k}_\perp , rapidity ν , spin s and color a . The inner product $(\cdot | \cdot)$ in this formula is defined by

$$\left(\widehat{\psi}_1 | \widehat{\psi}_2 \right)_\tau = \int d^2\mathbf{x}_\perp d\eta \widehat{\psi}_1^\dagger(\tau, \mathbf{x}_\perp, \eta) \widehat{\psi}_2(\tau, \mathbf{x}_\perp, \eta). \quad (10)$$

Because the background field is invariant under boosts in the direction of the collision, the squared inner product in eq. (9) produces two powers of $2\pi\delta(\nu - \nu')$. One of them is absorbed by the integral over $d\nu$, while the second power becomes a factor $2\pi\delta(0) \equiv L_\eta$, that precisely cancels the prefactor L_η^{-1} (unsurprisingly, since we are calculating the spectrum per unit of rapidity, the length of the rapidity interval under consideration must cancel from the result).

At very small proper time, the explicit form of the spinors involved in eq. (9) was derived in [18]. They read

$$\begin{aligned} \widehat{\psi}_{\mathbf{p}_\perp \nu s a}^{0+}(x) = & e^{-\pi i/4} \sqrt{\frac{2}{M_{\mathbf{p}}}} e^{i(\mathbf{p}_\perp \cdot \mathbf{x}_\perp + \nu\eta)} \left\{ e^{\pi\nu/2} \left(\frac{M_{\mathbf{p}}\tau}{2} \right)^{-i\nu} \Gamma\left(\frac{1}{2} + i\nu\right) \mathcal{P}^+ \right. \\ & \left. + e^{-\pi\nu/2} \left(\frac{M_{\mathbf{p}}\tau}{2} \right)^{i\nu} \Gamma\left(\frac{1}{2} - i\nu\right) \mathcal{P}^- \right\} u_s(\mathbf{p}_\perp, y=0) \chi_a \end{aligned} \quad (11)$$

and

$$\begin{aligned} \widehat{\psi}_{\mathbf{k}_\perp \nu s a}^-(x) = & -\frac{e^{\pi i/4}}{\sqrt{M_{\mathbf{k}}}} \int \frac{d^2\boldsymbol{\ell}_\perp}{(2\pi)^2} \frac{e^{i(\boldsymbol{\ell}_\perp \cdot \mathbf{x}_\perp + \nu\eta)}}{M_{\boldsymbol{\ell}}} \\ & \times \left\{ e^{\pi\nu/2} \left(\frac{M_{\boldsymbol{\ell}}^2\tau}{2M_{\mathbf{k}}} \right)^{i\nu} \Gamma\left(\frac{1}{2} - i\nu\right) U_2^\dagger(\mathbf{x}_\perp) \widetilde{U}_2(\boldsymbol{\ell}_\perp + \mathbf{k}_\perp) \gamma^+ \right. \\ & \left. + e^{-\pi\nu/2} \left(\frac{M_{\boldsymbol{\ell}}^2\tau}{2M_{\mathbf{k}}} \right)^{-i\nu} \Gamma\left(\frac{1}{2} + i\nu\right) U_1^\dagger(\mathbf{x}_\perp) \widetilde{U}_1(\boldsymbol{\ell}_\perp + \mathbf{k}_\perp) \gamma^- \right\} \\ & \times (\ell^i \gamma^i + m) v_s(\mathbf{k}_\perp, y=0) \chi_a, \end{aligned} \quad (12)$$

where χ_a ($a = 1, 2, 3$) is a unit vector in color space, $\mathcal{P}^+ \equiv (\gamma^- \gamma^+)/2$ and $\mathcal{P}^- \equiv (\gamma^+ \gamma^-)/2$ are projectors acting on the Dirac indices, $M_{\mathbf{k}} \equiv \sqrt{\mathbf{k}_\perp^2 + m^2}$ and $\tilde{U}_m(\mathbf{p}_\perp)$ is the Fourier transform of the Wilson line defined in eq. (2),

$$\tilde{U}_m(\boldsymbol{\ell}_\perp) = \int d^2 \mathbf{x}_\perp e^{-i \boldsymbol{\ell}_\perp \cdot \mathbf{x}_\perp} U_m(\mathbf{x}_\perp). \quad (13)$$

Eq. (9) is valid only if there is no background color field present at the time where the quark spectrum is evaluated. In particular, this formula is not gauge invariant because the expression (11) of the free spinor must be modified if there is a pure gauge (i.e. gauge equivalent to the null color field) background field. Let us ignore this difficulty for a brief moment, in order to see the type of pathology that one would encounter by using eq. (9) unmodified. For the setup of background field introduced in the previous section, we have

$$U_m(\mathbf{x}_\perp) = \frac{1 + \sigma^m}{2} e^{i \mathbf{Q}_m \cdot \mathbf{x}_\perp} + \frac{1 - \sigma^m}{2} e^{-i \mathbf{Q}_m \cdot \mathbf{x}_\perp} \quad (14)$$

and the Fourier transform reads

$$\tilde{U}_m(\boldsymbol{\ell}_\perp) = \frac{1 + \sigma^m}{2} (2\pi)^2 \delta^2(\boldsymbol{\ell}_\perp - \mathbf{Q}_m) + \frac{1 - \sigma^m}{2} (2\pi)^2 \delta^2(\boldsymbol{\ell}_\perp + \mathbf{Q}_m). \quad (15)$$

Plugging this in the dressed spinor (12) gives

$$\begin{aligned} \widehat{\psi}_{\mathbf{k}_\perp \nu sa}^-(x) &= \frac{e^{\pi i/4}}{\sqrt{M_{\mathbf{k}}}} e^{i(\nu \eta - \mathbf{k}_\perp \cdot \mathbf{x}_\perp)} \\ &\times \left\{ e^{\pi \nu/2} \Gamma\left(\frac{1}{2} - i\nu\right) \left[\frac{1}{M_{\mathbf{k} - \mathbf{Q}_2}} \left(\frac{M_{\mathbf{k} - \mathbf{Q}_2}^2 \tau}{2M_{\mathbf{k}}} \right)^{i\nu} \gamma^+ (M_{\mathbf{k}} \gamma^0 - Q_2^i \gamma^i) \frac{1 + \sigma^2}{2} \right. \right. \\ &\quad \left. \left. + \frac{1}{M_{\mathbf{k} + \mathbf{Q}_2}} \left(\frac{M_{\mathbf{k} + \mathbf{Q}_2}^2 \tau}{2M_{\mathbf{k}}} \right)^{i\nu} \gamma^+ (M_{\mathbf{k}} \gamma^0 + Q_2^i \gamma^i) \frac{1 - \sigma^2}{2} \right] \right. \\ &+ e^{-\pi \nu/2} \Gamma\left(\frac{1}{2} + i\nu\right) \left[\frac{1}{M_{\mathbf{k} - \mathbf{Q}_1}} \left(\frac{M_{\mathbf{k} - \mathbf{Q}_1}^2 \tau}{2M_{\mathbf{k}}} \right)^{-i\nu} \gamma^- (M_{\mathbf{k}} \gamma^0 - Q_1^i \gamma^i) \frac{1 + \sigma^1}{2} \right. \\ &\quad \left. \left. + \frac{1}{M_{\mathbf{k} + \mathbf{Q}_1}} \left(\frac{M_{\mathbf{k} + \mathbf{Q}_1}^2 \tau}{2M_{\mathbf{k}}} \right)^{-i\nu} \gamma^- (M_{\mathbf{k}} \gamma^0 + Q_1^i \gamma^i) \frac{1 - \sigma^1}{2} \right] \right\} \\ &\quad \times v_s(\mathbf{k}_\perp, y = 0) \chi_a. \quad (16) \end{aligned}$$

(In the derivation, we have used $(M_{\mathbf{k}} \gamma^0 - k^i \gamma^i + m) v_s(\mathbf{k}_\perp, y = 0) = 0$.) It is then straightforward to calculate the inner product between this spinor and the vacuum

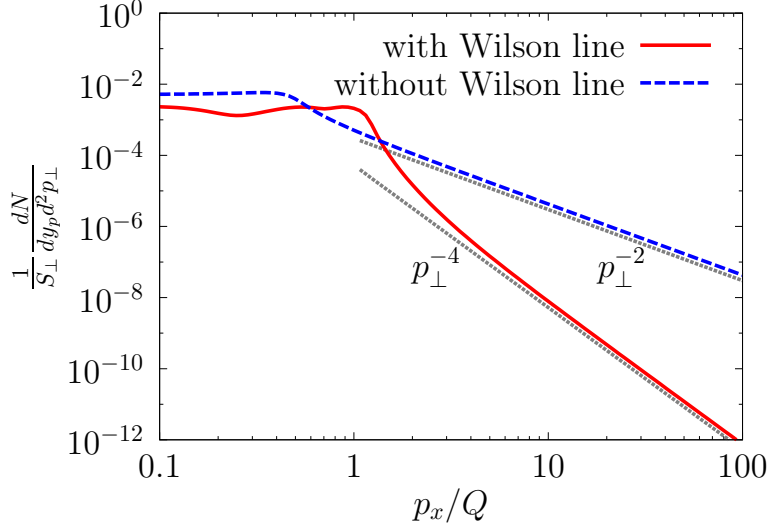


Figure 1: Quark spectrum (for $p_y = 0$, plotted as a function of p_x) in the purely electrical case (\mathbf{Q}_1 and \mathbf{Q}_2 parallel), for $Q_1 = Q_2 = Q_s/2$ and $m/Q_s = 0.1$. Dashed blue line: spectrum defined without a Wilson line. Solid red line: spectrum defined with a Wilson line. Dotted lines: power laws p_\perp^{-2} and p_\perp^{-4} .

spinor (11) in order to obtain the following expression of the quark spectrum,

$$\begin{aligned} \frac{dN}{dy_p d^2 \mathbf{p}_\perp} &= \frac{S_\perp}{8\pi^4} \left\{ 4 - \sum_{\epsilon_1, \epsilon_2 = \pm} \frac{F\left(\frac{M_{\mathbf{p}+\epsilon_1 \mathbf{Q}_1} M_{\mathbf{p}+\epsilon_2 \mathbf{Q}_2}}{M_p^2}\right)}{M_{\mathbf{p}+\epsilon_1 \mathbf{Q}_1} M_{\mathbf{p}+\epsilon_2 \mathbf{Q}_2}} \right. \\ &\quad \left. \times \left[M_p^2 - \epsilon_1 \epsilon_2 \mathbf{Q}_1 \cdot \mathbf{Q}_2 + \epsilon_1 \mathbf{p}_\perp \cdot \mathbf{Q}_1 + \epsilon_2 \mathbf{p}_\perp \cdot \mathbf{Q}_2 + 2\epsilon_1 \epsilon_2 \frac{(\mathbf{p}_\perp \cdot \mathbf{Q}_1)(\mathbf{p}_\perp \cdot \mathbf{Q}_2)}{M_p^2} \right] \right\}, \end{aligned} \quad (17)$$

with $F(x) \equiv \ln(x)/\sinh(\ln x)$ and S_\perp the transverse section of the overlap region of the colliding nuclei (this comes from a factor $(2\pi)^2 \delta(\mathbf{p}_\perp = 0)$). If we expand this expression at large transverse momentum ($p_\perp \gg Q_{1,2}$), the leading term is of the form

$$\frac{dN}{dy_p d^2 \mathbf{p}_\perp} \sim S_\perp \left\{ \frac{Q_1^2}{p_\perp^2} \oplus \frac{Q_2^2}{p_\perp^2} \right\}. \quad (18)$$

The spectrum (17) is plotted in figure 1 by the dashed line. Such a result suffers from two pathologies:

- Although it vanishes if $\mathbf{Q}_1 = \mathbf{Q}_2 = 0$, it does not vanish if only one of the vectors $\mathbf{Q}_{1,2}$ is zero. Physically, this means that this formula fails to give a null spectrum when one of the projectiles carries no color charge.
- The power law p_\perp^{-2} is inconsistent with expectations from perturbation theory (i.e. an order-by-order expansion in the color charge densities of the projectiles – see for instance [27, 24, 28]), that indicate that the spectrum should decrease as the fourth power of transverse momentum, p_\perp^{-4} .

The two problems are in fact related by a simple dimensional argument. Indeed, if we take for granted the proportionality of the spectrum to the transverse area S_\perp (a trivial consequence of the inclusive nature of the spectrum), the only way to increase the order in $\mathbf{Q}_{1,2}$ in the numerator (in order to have a term in $\mathbf{Q}_1^2 \mathbf{Q}_2^2$) is to also increase by two units the power in the denominator.

4 Effect of a straight Wilson line

4.1 Insertion of a Wilson line

As already mentioned, the main problem with the formula (9), regardless of the precise background field for which it is used, is that it assumes that the free positive energy spinors $\widehat{\psi}^{0+}$ are the vacuum ones. In particular, this implies a trivial color structure for the bilinear form constructed with this spinor,

$$\sum_{a'} \widehat{\psi}_{\mathbf{p}_\perp \nu' s' a'}^{0+}(x) \left[\widehat{\psi}_{\mathbf{p}_\perp \nu' s' a'}^{0+}(y) \right]^\dagger \propto \sum_{a'} \chi_{a'} \chi_{a'}^\dagger = \mathbf{1}_{\text{color}}. \quad (19)$$

If we perform a gauge rotation of all the color fields and spinors in the problem, the spectrum of produced quarks (summed over colors) should remain unchanged, but this can only be true if we replace eq. (11) by an expression that depends on the gauge rotated background field. As explained in [18], when the background field is a pure gauge, this dressing is achieved in a non-ambiguous manner by inserting a Wilson line connecting the two spinors. This amounts to the following replacement,

$$\sum_{a'} \chi_{a'} \chi_{a'}^\dagger \quad \rightarrow \quad W_\gamma(x, y), \quad (20)$$

where $W_\gamma(x, y)$ is a Wilson line between the points x and y , defined along a path γ . Note that this Wilson line can be taken to be along a purely spatial path since the quark spectrum involves a pair of spinors evaluated at equal times. Furthermore, since $A_\eta = -\tau^2 A^\eta = 0$ at $\tau = 0^+$, the measure $dx^\mu A_\mu$ does not receive any contribution from the rapidity direction (this statement is only true at the time $\tau = 0^+$, that we

consider here), and W_γ depends only on the projection of the path γ on the transverse plane.

When the background field at the time where the spectrum is evaluated is a pure gauge, such a Wilson line depends only on its endpoints, and the resulting spectrum is therefore non-ambiguous in the sense that it does not depend on the specific choice of the path γ . However, this is not the case in the MV model at a finite proper time, and in particular with the fields of eqs. (7) (that these fields are not a pure gauge is a trivial consequence of the fact that the \mathbf{E}, \mathbf{B} fields are not both zero – see eqs. (8)). Therefore, we expect a path dependence of the quark spectrum when evaluated after the substitution of eq. (20). In order to study this path dependence, one may first rewrite the quark spectrum in terms of the Fourier transform of the Wilson line W_γ as follows,

$$\frac{dN}{dy_p d^2 \mathbf{p}_\perp} = \frac{2}{(2\pi)^4} \int \frac{d^2 \mathbf{k}_\perp}{(2\pi)^2} \left\{ 2 \operatorname{tr}[\widetilde{W}_\gamma(\mathbf{k}_\perp)] - \frac{1}{2} \sum_{\epsilon_1, \epsilon_2 = \pm} G(\mathbf{p}_\perp, \mathbf{k}_\perp, \epsilon_1 \mathbf{Q}_1, \epsilon_2 \mathbf{Q}_2) \operatorname{tr} \left[(1 + \epsilon_1 \sigma^1 + \epsilon_2 \sigma^2) \widetilde{W}_\gamma(\mathbf{k}_\perp) \right] \right\}, \quad (21)$$

where

$$G(\mathbf{p}_\perp, \mathbf{k}_\perp, \mathbf{Q}_1, \mathbf{Q}_2) \equiv \frac{F\left(\frac{M_{\mathbf{k}-\mathbf{p}-\mathbf{Q}_1} M_{\mathbf{k}-\mathbf{p}-\mathbf{Q}_2}}{M_{\mathbf{p}} M_{\mathbf{k}-\mathbf{p}}}\right)}{M_{\mathbf{p}} M_{\mathbf{k}-\mathbf{p}} M_{\mathbf{k}-\mathbf{p}-\mathbf{Q}_1} M_{\mathbf{k}-\mathbf{p}-\mathbf{Q}_2}} \times \left[(M_{\mathbf{k}-\mathbf{p}}^2 - (\mathbf{k}_\perp - \mathbf{p}_\perp) \cdot \mathbf{k}_\perp) (M_{\mathbf{k}-\mathbf{p}}^2 - \mathbf{Q}_1 \cdot \mathbf{Q}_2) + (\mathbf{p}_\perp \cdot \mathbf{Q}_1) (M_{\mathbf{k}-\mathbf{p}}^2 - (\mathbf{k}_\perp - \mathbf{p}_\perp) \cdot \mathbf{Q}_2) + (\mathbf{p}_\perp \cdot \mathbf{Q}_2) (M_{\mathbf{k}-\mathbf{p}}^2 - (\mathbf{k}_\perp - \mathbf{p}_\perp) \cdot \mathbf{Q}_1) \right]. \quad (22)$$

($F(x)$ is the same function as in eq. (17).) and

$$\widetilde{W}_\gamma(\mathbf{k}_\perp) \equiv \int d^2 \mathbf{x}_\perp d^2 \mathbf{y}_\perp e^{i \mathbf{k}_\perp \cdot (\mathbf{x}_\perp - \mathbf{y}_\perp)} W_\gamma(\mathbf{x}_\perp, \mathbf{y}_\perp). \quad (23)$$

Note that when we do not insert the Wilson line W_γ (i.e., $W_\gamma \equiv \mathbf{1}_{\text{color}}$ and $\widetilde{W}_\gamma(\mathbf{k}_\perp) = S_\perp(2\pi)^2 \delta(\mathbf{k}_\perp) \times \mathbf{1}_{\text{color}}$), we recover the expression (17). The momentum integral in (21) can be performed analytically in the case of a purely electric background (\mathbf{Q}_1 parallel to \mathbf{Q}_2) as explained in Appendix B. For a purely electrical background, we do not need to specify the shape of the path used to defined the Wilson line, so this question can be postponed until later. The result is shown by the solid red line in the figure 1, where we can see that the tail of the quark spectrum now decreases

as p_\perp^{-4} . In the rest of this section, we consider a straight path γ , and provide an analytical explanation for this improved high- p_\perp behavior for general configurations of the vectors $\mathbf{Q}_{1,2}$.

4.2 Asymptotic expansion of the spectrum

In order to check whether the Wilson line W_γ fixes the incorrect large p_\perp behavior of the spectrum, we need a systematic way of obtaining the asymptotic expansion of eq. (21). Intuitively, large transverse momenta p_\perp should correspond to a small separation $\mathbf{x}_\perp - \mathbf{y}_\perp$, and we thus expect that this asymptotic expansion can be written in terms of the coefficients of the expansion of the Wilson line in powers of $\mathbf{x}_\perp - \mathbf{y}_\perp$. Firstly, we write

$$G(\mathbf{p}_\perp, \mathbf{k}_\perp, \mathbf{Q}_1, \mathbf{Q}_2) = 1 - \sum_{n \geq 2} \frac{1}{p_\perp^n} G^{(n)}(\hat{\mathbf{p}}_\perp, \mathbf{k}_\perp, \mathbf{Q}_1, \mathbf{Q}_2), \quad (24)$$

where $\hat{\mathbf{p}}_\perp \equiv \mathbf{p}_\perp/p_\perp$. (Note that the expansion of the function G has no term of order p_\perp^{-1} .) The zeroth order term cancels trivially with the term in $2 \text{tr}[\widetilde{W}_\gamma(\mathbf{k}_\perp)]$ in eq. (21). The remaining terms in the quark spectrum can be written as

$$\begin{aligned} \frac{dN}{dy_p d^2 \mathbf{p}_\perp} &= \frac{1}{(2\pi)^4} \sum_{n \geq 2} \frac{1}{p_\perp^n} \sum_{\epsilon_1, \epsilon_2 = \pm} \\ &\times \int \frac{d^2 \mathbf{k}_\perp}{(2\pi)^2} \text{tr} \left[G^{(n)}(\hat{\mathbf{p}}_\perp, \mathbf{k}_\perp, \epsilon_1 \mathbf{Q}_1, \epsilon_2 \mathbf{Q}_2) (1 + \epsilon_1 \sigma^1 + \epsilon_2 \sigma^2) \widetilde{W}_\gamma(\mathbf{k}_\perp) \right]. \end{aligned} \quad (25)$$

The explicit form of the coefficient functions $G^{(n)}$ that appear in this expansion are listed in the appendix A. These coefficients are polynomials in the components of the momentum \mathbf{k}_\perp , and therefore we need moments of the form

$$\int \frac{d^2 \mathbf{k}_\perp}{(2\pi)^2} k_\perp^{i_1} \cdots k_\perp^{i_n} \widetilde{W}_\gamma(\mathbf{k}_\perp). \quad (26)$$

This is where a dependence on the choice of the path γ may arise. Note however that the zeroth order moment is universal, since

$$\int \frac{d^2 \mathbf{k}_\perp}{(2\pi)^2} \widetilde{W}_\gamma(\mathbf{k}_\perp) = S_\perp \times \mathbf{1}_{\text{color}} \quad (27)$$

regardless of the path γ (this result is also true if we do not insert a Wilson line to connect the two spinors). If there is no Wilson line, all higher moments are identically zero, which gives the leading term in p_\perp^{-2} obtained in the previous section.

4.3 Leading term with a straight Wilson line

These moments are easiest to calculate when we choose a straight line to connect the points x and y . This path will provide a reference result to compare with when we consider curved paths in the next section. Let us denote W_L this straight Wilson line. Since the background color fields are homogeneous with our setup, this Wilson line has a trivial expression in coordinate space

$$W_L(\mathbf{x}_\perp, \mathbf{y}_\perp) = \exp(-ig\mathbf{A}_\perp \cdot (\mathbf{x}_\perp - \mathbf{y}_\perp)), \quad (28)$$

with $g\mathbf{A}_\perp \equiv \mathbf{Q}_1\sigma^1 + \mathbf{Q}_2\sigma^2$. The first moment of \widetilde{W}_L reads

$$\begin{aligned} \int \frac{d^2\mathbf{k}_\perp}{(2\pi)^2} k_\perp^i \widetilde{W}_L(\mathbf{k}_\perp) &= \int \frac{d^2\mathbf{k}_\perp}{(2\pi)^2} k_\perp^i \int d^2\mathbf{x}_\perp d^2\mathbf{y}_\perp e^{i\mathbf{k}_\perp \cdot (\mathbf{x}_\perp - \mathbf{y}_\perp)} W_\gamma(\mathbf{x}_\perp, \mathbf{y}_\perp) \\ &= S_\perp \int \frac{d^2\mathbf{k}_\perp}{(2\pi)^2} k_\perp^i \int d^2\mathbf{x}_\perp e^{i\mathbf{k}_\perp \cdot \mathbf{x}_\perp} W_\gamma(\mathbf{x}_\perp, 0) \\ &= S_\perp g A_\perp^i. \end{aligned} \quad (29)$$

For moments of order two and higher, the calculation is the same, but we have to pay attention to the non-commutative nature of \mathbf{A}_\perp . A careful analysis shows that one gets symmetrized products of the \mathbf{A}_\perp 's,

$$\int \frac{d^2\mathbf{k}_\perp}{(2\pi)^2} k_\perp^{i_1} \cdots k_\perp^{i_n} \widetilde{W}_L(\mathbf{k}_\perp) = \frac{S_\perp}{n!} \left\{ (gA_\perp^{i_1}) \cdots (gA_\perp^{i_n}) + \text{permutations} \right\}. \quad (30)$$

These products are then weighted by a factor $(1 + \epsilon_1\sigma^1 + \epsilon_2\sigma^2)$ and a color trace is performed. This gives the following replacement rules

$$\begin{aligned} 1 &\rightarrow 2 \\ k_\perp^i &\rightarrow 2(\epsilon_1 Q_1^i + \epsilon_2 Q_2^i) \\ k_\perp^i k_\perp^j &\rightarrow 2(Q_1^i Q_1^j + Q_2^i Q_2^j) \\ k_\perp^i k_\perp^j k_\perp^l &\rightarrow \frac{2}{3!} \left\{ (Q_1^i Q_1^j + Q_2^i Q_2^j) (\epsilon_1 Q_1^l + \epsilon_2 Q_2^l) + \text{perms.} \right\} \\ k_\perp^i k_\perp^j k_\perp^l k_\perp^m &\rightarrow \frac{2}{4!} \left\{ (Q_1^i Q_1^j + Q_2^i Q_2^j) (Q_1^l Q_1^m + Q_2^l Q_2^m) + \text{perms.} \right\} \end{aligned} \quad (31)$$

For the terms in p_\perp^{-2} , this leads to a coefficient of the form

$$\begin{aligned} \int \frac{d^2\mathbf{k}_\perp}{(2\pi)^2} \text{tr} \left[G^{(2)}(\widehat{\mathbf{p}}_\perp, \mathbf{k}_\perp, \epsilon_1 \mathbf{Q}_1, \epsilon_2 \mathbf{Q}_2) (1 + \epsilon_1\sigma^1 + \epsilon_2\sigma^2) \widetilde{W}_\gamma(\mathbf{k}_\perp) \right] \\ = -2\epsilon_1\epsilon_2 S_\perp \left(\mathbf{Q}_1 \cdot \mathbf{Q}_2 - \frac{2}{3} (\widehat{\mathbf{p}}_\perp \cdot \mathbf{Q}_1) (\widehat{\mathbf{p}}_\perp \cdot \mathbf{Q}_2) \right), \end{aligned} \quad (32)$$

which gives zero after summation over $\epsilon_{1,2} = \pm$. Note that this cancellation results from a delicate interplay between constant terms, terms in k_{\perp}^i , and terms in $k_{\perp}^i k_{\perp}^j$. At the order p_{\perp}^{-3} , even though the expressions are lengthier (see the appendix A), it turns out that the cancellation happens order by order in k_{\perp}^i , without the need of combining terms of various orders. The first non-canceling contributions arise at order p_{\perp}^{-4} (we have used MATHEMATICA to extract them, and do not provide here the explicit form of the coefficient $G^{(4)}$, which is rather unilluminating). At this order, the quark spectrum reads

$$\begin{aligned} \frac{dN}{dy_p d^2 \mathbf{p}_{\perp}} = \frac{S_{\perp}}{60\pi^4 p_{\perp}^4} & \left[27 \mathbf{Q}_1^2 \mathbf{Q}_2^2 - 12 (\mathbf{Q}_1 \cdot \mathbf{Q}_2)^2 - 8 (\hat{\mathbf{p}}_{\perp} \cdot \mathbf{Q}_1)^2 (\hat{\mathbf{p}}_{\perp} \cdot \mathbf{Q}_2)^2 \right. \\ & + 4 (\mathbf{Q}_1 \cdot \mathbf{Q}_2) (\hat{\mathbf{p}}_{\perp} \cdot \mathbf{Q}_1) (\hat{\mathbf{p}}_{\perp} \cdot \mathbf{Q}_2) \\ & \left. - 2 (\hat{\mathbf{p}}_{\perp} \cdot \mathbf{Q}_1)^2 \mathbf{Q}_2^2 - 2 (\hat{\mathbf{p}}_{\perp} \cdot \mathbf{Q}_2)^2 \mathbf{Q}_1^2 \right] + \mathcal{O}(p_{\perp}^{-5}). \end{aligned} \quad (33)$$

One may easily check that the coefficient of the term in p_{\perp}^{-4} is positive definite, for all orientations of the vectors $\hat{\mathbf{p}}_{\perp}$, \mathbf{Q}_1 and \mathbf{Q}_2 . Therefore, the conclusion of this section is that the insertion of a straight Wilson line removes the unphysical p_{\perp}^{-2} and p_{\perp}^{-3} terms from the quark spectrum.

5 Curved Wilson lines

5.1 Non-Abelian Stokes theorem

After having observed that the insertion of a straight Wilson line in the quark spectrum leads to an asymptotic behavior in agreement with perturbative expectations, the obvious question is that of the universality of this result:

- does the cancellation of the terms in p_{\perp}^{-2} and p_{\perp}^{-3} rely on taking a straight path between the two points?
- even if this cancellation works for any path γ , does the leading p_{\perp}^{-4} depend on the shape of the path?
- more generally, what is the lowest order at which a path dependence appears?

In order to address these questions, we need to compare the effect of Wilson lines defined on two different contours γ_1 and γ_2 . This can be done by considering the quantity $W_{\gamma_1} W_{\gamma_2}^{-1}$, which is a Wilson loop going from x to y along γ_1 and returning to x via γ_2 . In the Abelian case, this Wilson loop would be easily expressible in terms of the flux of the magnetic field through the loop, thanks to Stokes theorem. In a non-Abelian theory, the situation is more complicated because the magnetic field is

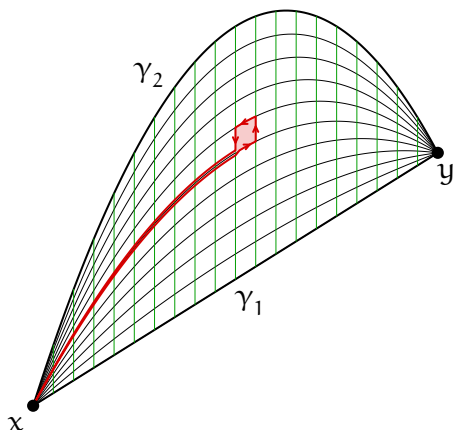


Figure 2: Illustration of the non-Abelian Stokes theorem. The argument of the exponential in eq. (35) is a sum of terms such as the one highlighted in red.

a non-commuting object, but there is a formal “non-Abelian Stokes theorem” that can be expressed as follows [29]. First, we define a family of curves $\gamma^\mu(t, s)$ that interpolate between γ_1 and γ_2 ,

$$\begin{aligned}\gamma^\mu(t, 0) &= \gamma_1^\mu(0) = \gamma_2^\mu(0) = x^\mu, \\ \gamma^\mu(t, 1) &= \gamma_1^\mu(1) = \gamma_2^\mu(1) = y^\mu, \\ \gamma^\mu(0, s) &= \gamma_1^\mu(s), \quad \gamma^\mu(1, s) = \gamma_2^\mu(s).\end{aligned}\tag{34}$$

In words, t is a parameter that labels the curves interpolating between γ_1 and γ_2 , while s is a coordinate that labels the points along each of these curves. The non-Abelian Stokes theorem reads (see the figure 2 for an illustration)

$$W_{\gamma_1} W_{\gamma_2}^{-1} = P_t \exp \left\{ ig \int_0^1 dt ds \frac{\partial \gamma^\mu}{\partial t} \frac{\partial \gamma^\nu}{\partial s} W_{\gamma(t, \cdot)}(0, s) F_{\mu\nu}(\gamma(s, t)) W_{\gamma(t, \cdot)}^{-1}(0, s) \right\}, \tag{35}$$

where $W_{\gamma(t, \cdot)}(0, s)$ denotes the Wilson that goes from x^μ to $\gamma^\mu(s, t)$ along the path $\gamma^\mu(t, \cdot)$. Note that the ordering of the exponential in this formula applies only to the t integral (the ordering in s is fully specified by the Wilson lines $W_{\gamma(t, \cdot)}(0, s)$). Under a gauge transformation Ω , the combination $W_{\gamma(t, \cdot)}(0, s) F_{\mu\nu}(\gamma(s, t)) W_{\gamma(t, \cdot)}^{-1}(0, s)$ transforms as

$$W_{\gamma(t, \cdot)}(0, s) F_{\mu\nu}(\gamma(s, t)) W_{\gamma(t, \cdot)}^{-1}(0, s) \rightarrow \Omega(x) W_{\gamma(t, \cdot)}(0, s) F_{\mu\nu}(\gamma(s, t)) W_{\gamma(t, \cdot)}^{-1}(0, s) \Omega^\dagger(x), \tag{36}$$

which is precisely the expected transformation of the Wilson loop $W_{\gamma_1} W_{\gamma_2}^{-1}$. We see the crucial role played by the Wilson lines $W_{\gamma(t,\cdot)}(0, s)$ in obtaining the correct transformation law. We can also foresee that these Wilson lines lead to a crucial difference between the Abelian and non-Abelian cases regarding the behavior of a small Wilson loop. In the Abelian case, a small Wilson loop depends only on the magnetic flux through the loop, i.e. on the local magnetic field and on the area of the loop. In the non-Abelian case, the presence of $W_{\gamma(t,\cdot)}(0, s)$ implies also a dependence upon the length of the paths connecting x to other points inside the loop.

In the case of interest here, where the paths $\gamma_{1,2}$ are embedded in the transverse plane, the only component of the field strength that enters in this formula is F_{12} , i.e. the component of the chromo-magnetic field in the z direction. A trivial consequence of this observation is that the paths γ_1 and γ_2 give the same Wilson line in the case where the background field is purely electrical (i.e. when $\mathbf{Q}_{1,2}$ are parallel). Thus, in this case, the quark spectrum defined by inserting a Wilson line does not depend on the shape of the path.

Let us now consider the general case. The Wilson line W_γ defined on an arbitrary path may be related to the linear one by writing

$$W_\gamma = (W_\gamma W_L^{-1}) W_L \quad (37)$$

and the factor $W_\gamma W_L^{-1}$ is a Wilson loop that can be expressed in terms of the transverse magnetic field and the gauge potentials $A^{1,2}$ thanks to the non-Abelian Stokes theorem. As we have seen in the previous section, the important quantities are the moments of the Fourier transform of the Wilson line, that are also the Taylor coefficients of its short distance expansion. Therefore, one way of assessing the effect of a curved Wilson line compared to a straight one is to study how the loop $W_\gamma W_L^{-1}$ behaves when $\mathbf{y}_\perp \rightarrow \mathbf{x}_\perp$. Despite its complicated structure, the non-Abelian Stokes formula is useful for estimating this behavior. Two parameters control this limit. Firstly, because $dt ds \frac{\partial \gamma^\mu}{\partial t} \frac{\partial \gamma^\nu}{\partial s}$ measures the area of an elementary element (e.g., the area of a little square in the figure 2) of the surface enclosed by the loop, there will be terms proportional to the area times the magnetic field transverse to the loop. Secondly, because of the Wilson lines $W_{\gamma(t,\cdot)}(0, s)$, there will be terms involving the gauge potential times the distance between \mathbf{x}_\perp and other points inside the loop. Because of this, we must distinguish several possibilities for the shape of the path. Three of them are illustrated in the figure 3, that we shall study in turn hereafter.

5.2 Paths with bounded curvature

The situation, shown on the left panel of the figure 3, which is closest to a straight line is a path whose curvature is bounded (i.e. whose radius of curvature is always

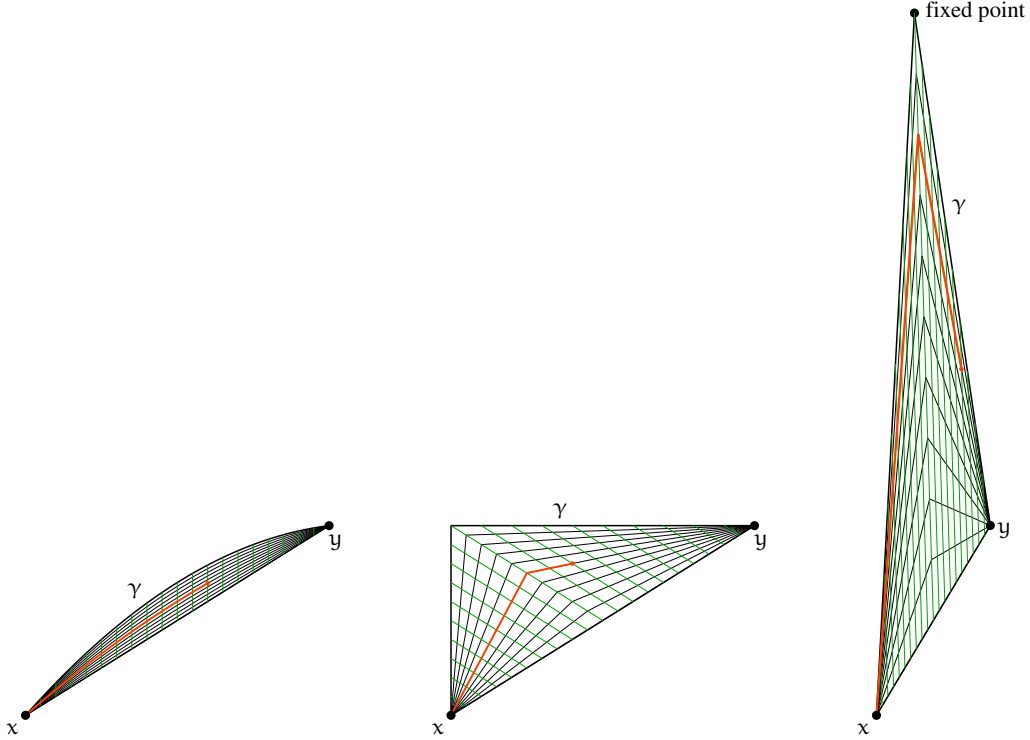


Figure 3: Examples of paths that have different area and length scalings when $\mathbf{y}_\perp \rightarrow \mathbf{x}_\perp$. Left: smooth path with bounded curvature. Middle: path with unbounded curvature and a length that goes to zero linearly. Right: path with length that does not vanish when $\mathbf{y}_\perp \rightarrow \mathbf{x}_\perp$. In orange, we have represented a typical Wilson line $W_{\gamma(t,\cdot)}(0, s)$ entering in the right hand side of eq. (35).

larger than some value R). For such a path, the area enclosed within the loop and the length of a typical Wilson line $W_{\gamma(t,\cdot)}(0, s)$ scale as

$$\text{Area} \sim \frac{\delta^3}{R}, \quad \text{Length} \sim \delta, \quad (38)$$

where $\delta \equiv |\mathbf{y}_\perp - \mathbf{x}_\perp|$. When $\delta \rightarrow 0$, the Wilson loop behaves as

$$W_\gamma W_L^{-1} = 1 \oplus \frac{\delta^3 B}{R} \sigma^3 \oplus \frac{\delta^4 B Q}{R} \sigma^3 \sigma^{1,2} \oplus \dots \quad (39)$$

In this formula, we have made explicit the fact that the longitudinal magnetic field is proportional to the color generator σ^3 . At the order δ^3 , we may replace by $\mathbf{1}$ the

Wilson line $W_{\gamma(t,\cdot)}(0, s)$ in the right hand side of eq. (35), because its length goes to zero as $\delta \rightarrow 0$. Deviations of this Wilson line from the identity contribute only to higher orders in the separation δ , e.g., the term in δ^4 in eq. (39), where Q denotes generically the magnitude of $\mathbf{Q}_{1,2}$. (Here, we use the fact that the components of the gauge potential A^i are proportional to the color generators σ^1 or σ^2 in our setup.) Likewise, the straight Wilson line behaves as

$$W_L = 1 \oplus \delta (Q\sigma^{1,2}) \oplus \delta^2 (Q\sigma^{1,2})^2 \oplus \dots \quad (40)$$

By multiplying eqs. (39) and (40), we get the following short distance behavior for a Wilson line with bounded curvature,

$$W_\gamma = \underbrace{1 \oplus \delta (Q\sigma^{1,2}) \oplus \delta^2 (Q\sigma^{1,2})^2 \oplus \dots}_{W_L} \oplus \frac{\delta^3 B}{R} \sigma^3 \oplus \underline{\frac{\delta^4 BQ}{R} \sigma^3 \sigma^{1,2}} \oplus \dots \quad (41)$$

The first line in the right hand side is the result for a straight Wilson line, studied more explicitly in the previous section. The second line displays the structure of the first two terms involving the magnetic flux (note that these terms all go to zero if $R \rightarrow \infty$, i.e. if the curvature of the path under consideration goes to zero). The first of these terms does not contribute, since it is proportional to σ^3 and only enters in the following color trace,

$$\text{tr} (\sigma^3 (1 + \epsilon_1 \sigma^1 + \epsilon_2 \sigma^2)) = 0. \quad (42)$$

The second of these terms (underlined in eq. (41)) does not suffer from this cancellation, since we have for instance

$$\text{tr} (\sigma^3 \sigma^1 (1 + \epsilon_1 \sigma^1 + \epsilon_2 \sigma^2)) = 2i\epsilon_2 \neq 0. \quad (43)$$

But note that this trace is proportional to ϵ_2 , and that there is a sum on $\epsilon_2 = \pm$ in the expression of the quark spectrum. Therefore, to obtain a non-null contribution, another power of ϵ_2 must arise from the coefficient function $G^{(n)}(\hat{\mathbf{p}}_\perp, \mathbf{k}_\perp, \epsilon_1 Q_1, \epsilon_2 Q_2)$. The generic structure of $G^{(n)}$ reads

$$G^{(n)}(\hat{\mathbf{p}}_\perp, \mathbf{k}_\perp, \epsilon_1 Q_1, \epsilon_2 Q_2) = k_\perp^n \oplus \underline{\epsilon Q k_\perp^{n-1}} \oplus \dots \oplus (\epsilon Q)^n. \quad (44)$$

But at the same time, recall that only terms with a degree in k_\perp equal to the order in δ can contribute, since we have seen that the p -th moments of the Fourier transform of the Wilson line are the Taylor coefficients of order p in its short distance expansion. We have underlined in the previous equation the term that gives the leading high- p_\perp

behavior. Since the underlined term in eq. (41) is of order δ^4 , we must have $n = 5$ to obtain a matching term of order k_\perp^4 , which means that the magnetic flux starts to contribute only at the order p_\perp^{-5} . Therefore, when the path defining the Wilson line has a bounded curvature, the leading term in the high- p_\perp quark spectrum is universal, i.e. insensitive to variations of the shape of the path. Schematically, the spectrum reads

$$\frac{dN}{dy_p d^2 \mathbf{p}_\perp} \underset{\text{bounded curvature}}{=} S_\perp \left\{ \underbrace{\frac{Q^4}{p_\perp^4}}_{\text{universal}} \oplus \underbrace{\frac{Q^2 B}{R p_\perp^5}}_{\text{path dependent}} \oplus \dots \right\}. \quad (45)$$

Note that $B \sim Q^2$. But we prefer to keep explicitly the dependence on the magnetic field, to stress the fact that the path dependent term does not exist if the background field is purely electrical.

5.3 Paths with unbounded curvature

From the formula (45), we see that path dependent term tends to grow when the radius of curvature decreases. As we shall now show, if the curvature is unbounded, the path dependence is in fact promoted at least one order earlier, at p_\perp^{-4} . In fact, there are two main classes of paths with unbounded curvature: those whose length goes to zero (linearly in δ) when $\delta \rightarrow 0$, and those whose length goes to a non-zero constant. Let us consider the first class of paths, illustrated in the middle panel of figure 3. In this case, we have

$$\text{Area} \sim \delta^2, \quad \text{Length} \sim \delta. \quad (46)$$

The reasoning is the same as in the previous subsection, but since the area scales as δ^2 instead of δ^3 , we need a term in $\epsilon Q k_\perp^3$ (instead of $\epsilon Q k_\perp^4$) in the final step. Such a term can be obtained in $G^{(4)}$, implying that the path dependence now appears at the order p_\perp^{-4} of the high- p_\perp spectrum,

$$\frac{dN}{dy_p d^2 \mathbf{p}_\perp} \underset{\text{unbounded curvature}}{=} S_\perp \left\{ \underbrace{\frac{Q^4}{p_\perp^4}}_{\text{universal}} \oplus \underbrace{\frac{Q^2 B}{p_\perp^4}}_{\text{path dependent}} \oplus \dots \right\}. \quad (47)$$

In Appendix C.1, we demonstrate that such a path-dependent p_\perp^{-4} tail actually appears for specific choices of paths that have unbounded curvature.

5.4 Paths going through a fixed point

Consider now paths such as the one shown in the right panel of figure 3, where γ always goes through a fixed point. In this case, we have

$$\text{Area} \sim \ell\delta, \quad \text{Length} \sim \ell, \quad (48)$$

where ℓ is the distance between \mathbf{x}_\perp and this fixed point. Since the length of the Wilson line $W_{\gamma(t,\cdot)}(0, s)$ does not go to zero, it contributes at a lower order than in the previous two cases. Now, we can write

$$W_\gamma W_L^{-1} = 1 \oplus \ell\delta B \sigma^3 \oplus \ell^2 \delta B Q \sigma^3 \sigma^{1,2} \oplus \dots \quad (49)$$

The third term in the right hand side, that comes from the expansion of $W_{\gamma(t,\cdot)}(0, s)$, has the same dependence on δ as the second term. From this, we get

$$W_\gamma = \underbrace{1 \oplus \delta (Q\sigma^{1,2}) \oplus \delta^2 (Q\sigma^{1,2})^2 \oplus \dots}_{W_L} \oplus \delta \ell B \sigma^3 \oplus \delta \ell^2 B Q \sigma^3 \sigma^{1,2} \oplus \dots \quad (50)$$

Note that the color structure of the underlined term leads to a non-zero trace. By the same reasoning as before, since this term is linear in δ , the adequate powers of k_\perp can be found in the coefficient function $G^{(2)}$. This means that for this type of path, the path dependence would start at the order p_\perp^{-2} , leading to an unphysically hard spectrum,

$$\frac{dN}{dy_p d^2 \mathbf{p}_\perp} \Big|_{\text{fixed point}} = S_\perp \left\{ \underbrace{\frac{\ell^2 Q^2 B}{p_\perp^2}}_{\text{path dependent}} \oplus \dots \right\}. \quad (51)$$

The occurrence of such a term in p_\perp^{-2} is illustrated in the figure 4, where the points \mathbf{x}_\perp and \mathbf{y}_\perp are connected by the piecewise linear path γ defined by $\mathbf{x}_\perp \equiv (x^1, x^2) \rightarrow (0, x^2) \rightarrow (0, 0) \rightarrow (0, y^2) \rightarrow \mathbf{y}_\perp \equiv (y^1, y^2)$. See Appendix C.2 for details.

6 Summary and conclusions

In this paper, we have used a special configuration of $SU(2)$ color currents in order to obtain an analytically tractable –at least up to $\tau = 0^+$, i.e. just after the collision has happened– model of two-nuclei collision in the CGC framework. Then, we evaluate the inclusive quark spectrum at $\tau = 0^+$ in the classical color field obtained in this setup. Firstly, we have showed that without including a Wilson line between the two

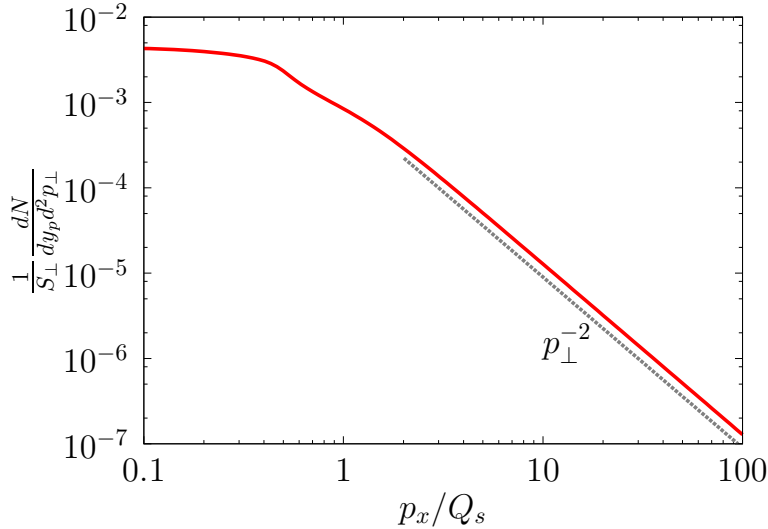


Figure 4: Quark spectrum defined with a Wilson line that goes through a fixed point, in the purely magnetic case ($\mathbf{Q}_1 \equiv \frac{1}{2}(0, Q_s)$, $\mathbf{Q}_2 \equiv \frac{1}{2}(Q_s, 0)$, $m/Q_s = 0.1$). Solid red line: the spectrum (69) as a function of p_x at $p_y = 0$. Grey dotted line: power law p_\perp^{-2} .

spinors, this spectrum has an unphysical tail in p_\perp^{-2} . Moreover, it does not vanish if we turn off the color current of only one projectile. If a Wilson line defined on a straight line connecting the two points is inserted, these pathologies can be shown to disappear: the spectrum now decreases as p_\perp^{-4} and vanishes when any of the currents is turned off.

Then, we have studied the dependence of the spectrum on the shape of the path, which influences the result when the background color field has a magnetic component in the z direction. In order to do this, we first expressed the successive terms of the asymptotic expansion of the spectrum in terms of the moments of the Fourier transform of the Wilson line. These moments are then related to the short distance expansion of the Wilson line in coordinate space. Using the non-Abelian Stokes theorem, we showed that this short distance behavior depends crucially on the shape of the path, notably on whether it has a bounded curvature or is allowed to have kinks.

When the curvature is bounded, our power counting shows that the first path dependent term is at most of order p_\perp^{-5} , implying that the leading p_\perp^{-4} term is shape independent. In this case, the tail of the spectrum $p_\perp \gtrsim Q_s$ is universal even in the presence of a non-pure gauge background field, but the softer part of the quark

spectrum may still suffer from an ambiguity related to the choice of the path defining the Wilson line.

In contrast, if the curvature is not bounded, the path dependence is promoted at least to order p_{\perp}^{-4} , or even to order p_{\perp}^{-2} if one considers a path that goes through a fixed point. This means that with such a contour, the entire spectrum –including the hard tail– would be path dependent. One should presumably avoid using such singular paths, since it seems that the unphysical features of the spectrum are a direct consequence of the non-analyticity of the path.

Let us end by some more speculative words. Although our study was done with a special configuration of the color sources of the projectiles, the fact that the shape of the path has a strong influence on the lowest order at which the path dependence arises is certainly robust. We thus expect that, for completely general color backgrounds, analytic curves are those that minimize the path dependence. Moreover, although we have considered the quark spectrum at a proper time $\tau = 0^+$ in this paper in order to be able to perform some analytical calculations, the same conclusions would hold for the spectrum evaluated at a later time. The only change would be that, thanks to the fact that the magnetic field decreases with time, the path dependence should progressively decrease as $Q_s\tau$ increases.

Acknowledgements

FG's work was supported by the Agence Nationale de la Recherche through the project ANR-16-CE31-0019-01.

A Asymptotic expansion of the function G

The first non-zero coefficient function, at the second order, reads

$$G^{(2)}(\hat{\mathbf{p}}_{\perp}, \mathbf{k}_{\perp}, \mathbf{Q}_1, \mathbf{Q}_2) = \frac{1}{2}(\mathbf{Q}_1 + \mathbf{Q}_2 - \mathbf{k}_{\perp})^2 - \frac{1}{3}[\hat{\mathbf{p}}_{\perp} \cdot (\mathbf{Q}_1 + \mathbf{Q}_2 - \mathbf{k}_{\perp})]^2. \quad (52)$$

Note that the result dependence of this coefficient on \mathbf{p}_{\perp} is only through the orientation of the transverse momentum, not its magnitude. At the third order, we can write

$$G^{(3)}(\hat{\mathbf{p}}_{\perp}, \mathbf{k}_{\perp}, \mathbf{Q}_1, \mathbf{Q}_2) \equiv G_0^{(3)}(\hat{\mathbf{p}}_{\perp}, \mathbf{k}_{\perp}, \mathbf{Q}_1, \mathbf{Q}_2) + G_1^{(3)}(\hat{\mathbf{p}}_{\perp}, \mathbf{k}_{\perp}, \mathbf{Q}_1, \mathbf{Q}_2) \\ + G_2^{(3)}(\hat{\mathbf{p}}_{\perp}, \mathbf{k}_{\perp}, \mathbf{Q}_1, \mathbf{Q}_2) + G_3^{(3)}(\hat{\mathbf{p}}_{\perp}, \mathbf{k}_{\perp}, \mathbf{Q}_1, \mathbf{Q}_2), \quad (53)$$

with

$$\begin{aligned}
& G_0^{(3)}(\hat{\mathbf{p}}_\perp, \mathbf{k}_\perp, \mathbf{Q}_1, \mathbf{Q}_2) \\
&= -\frac{1}{6} [6(\mathbf{Q}_1 \cdot \mathbf{Q}_2)(\hat{\mathbf{p}}_\perp \cdot \mathbf{Q}_1 + \hat{\mathbf{p}}_\perp \cdot \mathbf{Q}_2) \\
&\quad + (\hat{\mathbf{p}}_\perp \cdot \mathbf{Q}_1)(5\mathbf{Q}_1^2 - \mathbf{Q}_2^2) + (\hat{\mathbf{p}}_\perp \cdot \mathbf{Q}_2)(5\mathbf{Q}_2^2 - \mathbf{Q}_1^2)] \\
&\quad + \frac{2}{3} [(\hat{\mathbf{p}}_\perp \cdot \mathbf{Q}_1)^3 + (\hat{\mathbf{p}}_\perp \cdot \mathbf{Q}_2)^3 + (\hat{\mathbf{p}}_\perp \cdot \mathbf{Q}_1)^2(\hat{\mathbf{p}}_\perp \cdot \mathbf{Q}_2) + (\hat{\mathbf{p}}_\perp \cdot \mathbf{Q}_1)(\hat{\mathbf{p}}_\perp \cdot \mathbf{Q}_2)^2], \quad (54)
\end{aligned}$$

$$\begin{aligned}
& G_1^{(3)}(\hat{\mathbf{p}}_\perp, \mathbf{k}_\perp, \mathbf{Q}_1, \mathbf{Q}_2) \\
&= \frac{1}{6} [(12\mathbf{Q}_1 \cdot \mathbf{Q}_2 + 5\mathbf{Q}_1^2 + 5\mathbf{Q}_2^2)(\hat{\mathbf{p}}_\perp \cdot \mathbf{k}_\perp) \\
&\quad + (10\hat{\mathbf{p}}_\perp \cdot \mathbf{Q}_1 + 4\hat{\mathbf{p}}_\perp \cdot \mathbf{Q}_2)(\mathbf{Q}_1 \cdot \mathbf{k}_\perp) + (4\hat{\mathbf{p}}_\perp \cdot \mathbf{Q}_1 + 10\hat{\mathbf{p}}_\perp \cdot \mathbf{Q}_2)(\mathbf{Q}_2 \cdot \mathbf{k}_\perp)] \\
&\quad - \frac{2}{3} [3(\hat{\mathbf{p}}_\perp \cdot \mathbf{Q}_1)^2 + 3(\hat{\mathbf{p}}_\perp \cdot \mathbf{Q}_2)^2 + 4(\hat{\mathbf{p}}_\perp \cdot \mathbf{Q}_1)(\hat{\mathbf{p}}_\perp \cdot \mathbf{Q}_2)] (\hat{\mathbf{p}}_\perp \cdot \mathbf{k}_\perp), \quad (55)
\end{aligned}$$

$$\begin{aligned}
& G_2^{(3)}(\hat{\mathbf{p}}_\perp, \mathbf{k}_\perp, \mathbf{Q}_1, \mathbf{Q}_2) \\
&= -\frac{1}{6} [5(\hat{\mathbf{p}}_\perp \cdot \mathbf{Q}_1 + \hat{\mathbf{p}}_\perp \cdot \mathbf{Q}_2) \mathbf{k}_\perp^2 + 10(\hat{\mathbf{p}}_\perp \cdot \mathbf{k}_\perp)(\mathbf{Q}_1 \cdot \mathbf{k}_\perp + \mathbf{Q}_2 \cdot \mathbf{k}_\perp)] \\
&\quad + 2(\hat{\mathbf{p}}_\perp \cdot \mathbf{Q}_1 + \hat{\mathbf{p}}_\perp \cdot \mathbf{Q}_2) (\hat{\mathbf{p}}_\perp \cdot \mathbf{k}_\perp)^2, \quad (56)
\end{aligned}$$

and

$$G_3^{(3)}(\hat{\mathbf{p}}_\perp, \mathbf{k}_\perp, \mathbf{Q}_1, \mathbf{Q}_2) = \frac{5}{6}(\hat{\mathbf{p}}_\perp \cdot \mathbf{k}_\perp) \mathbf{k}_\perp^2 - \frac{2}{3}(\hat{\mathbf{p}}_\perp \cdot \mathbf{k}_\perp)^3. \quad (57)$$

The subscripts 0, 1, 2, 3 indicate the degree in \mathbf{k}_\perp of the corresponding terms. This organization is useful since it corresponds to the successive coefficients of the Wilson line at small separations $\mathbf{x}_\perp - \mathbf{y}_\perp$.

B Quark spectrum in a purely electric background

When the background field is purely electric, the quark spectrum (21) can be computed explicitly without relying on the asymptotic expansion in $1/p_\perp$. A purely electric background is realized if the two vectors \mathbf{Q}_1 and \mathbf{Q}_2 are parallel. In such a background, the Wilson line $W_\gamma(x, y)$ is independent of a path γ and only a function of $\mathbf{x}_\perp - \mathbf{y}_\perp$ as

$$W_\gamma(\mathbf{x}_\perp, \mathbf{y}_\perp) = \cos [\overline{\mathbf{Q}} \cdot (\mathbf{x}_\perp - \mathbf{y}_\perp)] - i \frac{Q_1 \sigma^1 + Q_2 \sigma^2}{\sqrt{Q_1^2 + Q_2^2}} \sin [\overline{\mathbf{Q}} \cdot (\mathbf{x}_\perp - \mathbf{y}_\perp)]. \quad (58)$$

Here, we denote $Q_{1,2} \equiv |\mathbf{Q}_{1,2}|$ and $\bar{\mathbf{Q}} \equiv \sqrt{Q_1^2 + Q_2^2} \mathbf{Q}_1/Q_1$. The Fourier transform (23) of this Wilson line is

$$\widetilde{W}_\gamma(\mathbf{k}_\perp) = \frac{1}{2} S_\perp \sum_{\lambda=\pm} \left(1 + \lambda \frac{Q_1 \sigma^1 + Q_2 \sigma^2}{\sqrt{Q_1^2 + Q_2^2}} \right) (2\pi)^2 \delta(\mathbf{k}_\perp - \lambda \bar{\mathbf{Q}}). \quad (59)$$

By plugging this expression into eq. (21), we find the quark spectrum in the purely electric background as

$$\frac{dN}{dy_p d^2 \mathbf{p}_\perp} = \frac{S_\perp}{(2\pi)^4} \sum_{\epsilon_1, \epsilon_2, \lambda=\pm} \left[1 - \left(1 + \lambda \frac{\epsilon_1 Q_1 + \epsilon_2 Q_2}{\sqrt{Q_1^2 + Q_2^2}} \right) G(\mathbf{p}_\perp, \lambda \bar{\mathbf{Q}}, \epsilon_1 \mathbf{Q}_1, \epsilon_2 \mathbf{Q}_2) \right]. \quad (60)$$

One can easily confirm that this spectrum vanishes when one of \mathbf{Q}_1 or \mathbf{Q}_2 is zero. In agreement with the general result (33), the high- p_\perp expansion of this spectrum starts with the order p_\perp^{-4} ,

$$\frac{dN}{dy_p d^2 \mathbf{p}_\perp} = \frac{S_\perp}{60\pi^4 p_\perp^4} [15Q_1^2 Q_2^2 - 8(\hat{\mathbf{p}}_\perp \cdot \mathbf{Q}_1)^2 (\hat{\mathbf{p}}_\perp \cdot \mathbf{Q}_2)^2] + \mathcal{O}(p_\perp^{-6}). \quad (61)$$

C Quark spectrum in a purely magnetic background

When the vectors \mathbf{Q}_1 and \mathbf{Q}_2 are not parallel, nonzero chromo-magnetic fields are generated after the collision. In the presence of a magnetic field, the Wilson line has a path-dependence and it is not easy in general to compute the Fourier transform of the Wilson line analytically. In this appendix, we consider a purely magnetic field configuration that is realized by

$$\mathbf{Q}_1 = (Q_1, 0), \quad \mathbf{Q}_2 = (0, Q_2), \quad (62)$$

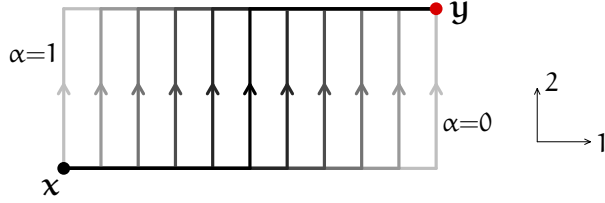
and derive explicit forms of the quark spectra for specific paths that allow analytic calculations.

C.1 Paths with unbounded curvature

First, we take a one-parameter family of paths which are piecewise linear,

$$\gamma_\alpha : \quad \mathbf{x}_\perp \equiv (x^1, x^2) \rightarrow (\alpha x^1 + (1-\alpha)y^1, x^2) \rightarrow (\alpha x^1 + (1-\alpha)y^1, y^2) \rightarrow \mathbf{y}_\perp \equiv (y^1, y^2),$$

with a varying parameter $\alpha \in [0, 1]$, as shown here:



The paths in this family have an unbounded curvature, but a length that goes to zero as $\mathbf{y}_\perp \rightarrow \mathbf{x}_\perp$. Therefore, according to the discussion presented in the section 5.3, we expect that the quark spectrum contains an α -dependent term of order p_\perp^{-4} . Using the shorthand notations $\Delta x^1 \equiv x^1 - y^1$ and $\Delta x^2 \equiv x^2 - y^2$, the Wilson line along this contour reads

$$\begin{aligned} W_{\gamma_\alpha}(\mathbf{x}_\perp, \mathbf{y}_\perp) &= e^{-i(1-\alpha)Q_1\sigma^1\Delta x^1} e^{-iQ_2\sigma^2\Delta x^2} e^{-i\alpha Q_1\sigma^1\Delta x^1} \\ &= \frac{1}{4} \sum_{\lambda_1, \lambda_2 = \pm} \left[(1 + \lambda_1\sigma^1) e^{-i\lambda_1 Q_1 \Delta x^1 - i\lambda_2 Q_2 \Delta x^2} \right. \\ &\quad \left. + \lambda_2(\sigma^2 + i\lambda_1\sigma^3) e^{-i\lambda_1(1-2\alpha)Q_1\Delta x^1 - i\lambda_2 Q_2 \Delta x^2} \right]. \end{aligned} \quad (63)$$

Its Fourier transform is

$$\begin{aligned} \widetilde{W}_{\gamma_\alpha}(\mathbf{k}_\perp) &= \frac{S_\perp}{4} \sum_{\lambda_1, \lambda_2 = \pm} \left[(1 + \lambda_1\sigma^1) (2\pi)^2 \delta(\mathbf{k}_\perp - \lambda_1 \mathbf{Q}_1 - \lambda_2 \mathbf{Q}_2) \right. \\ &\quad \left. + \lambda_2(\sigma^2 + i\lambda_1\sigma^3) (2\pi)^2 \delta(\mathbf{k}_\perp - \lambda_1(1-2\alpha)\mathbf{Q}_1 - \lambda_2 \mathbf{Q}_2) \right]. \end{aligned} \quad (64)$$

For this Wilson line, the quark spectrum (21) becomes

$$\begin{aligned} \frac{dN}{dy_p d^2 \mathbf{p}_\perp} &= \frac{S_\perp}{32\pi^4} \sum_{\epsilon_1, \epsilon_2, \lambda_1, \lambda_2 = \pm} \left[1 - (1 + \lambda_1 \epsilon_1) G(\mathbf{p}_\perp, \lambda_1 \mathbf{Q}_1 + \lambda_2 \mathbf{Q}_2, \epsilon_1 \mathbf{Q}_1, \epsilon_2 \mathbf{Q}_2) \right. \\ &\quad \left. - \lambda_2 \epsilon_2 G(\mathbf{p}_\perp, \lambda_1(1-2\alpha)\mathbf{Q}_1 + \lambda_2 \mathbf{Q}_2, \epsilon_1 \mathbf{Q}_1, \epsilon_2 \mathbf{Q}_2) \right]. \end{aligned} \quad (65)$$

The high- p_\perp asymptotic form of this spectrum is

$$\frac{dN}{dy_p d^2 \mathbf{p}_\perp} = \frac{S_\perp Q_1^2 Q_2^2}{60\pi^4 p_\perp^4} (25 - 8\widehat{p}_x^2 \widehat{p}_y^2) - \frac{S_\perp Q_1^2 Q_2^2}{15\pi^4 p_\perp^4} (2\alpha - 1)^2 (15 - 32\widehat{p}_x^2 \widehat{p}_y^2) + \mathcal{O}(p_\perp^{-6}). \quad (66)$$

This result is perfectly consistent with eq. (47). The first term of the right hand side corresponds to the universal term given in eq. (33), and the second term depends on

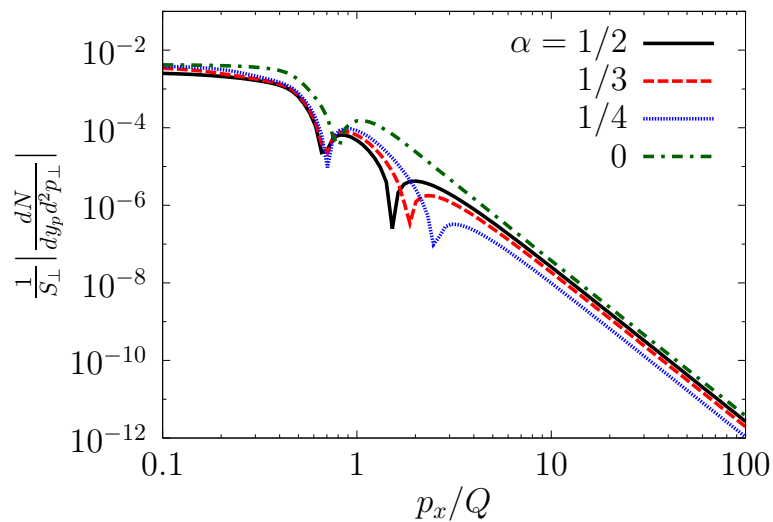


Figure 5: Comparison of the spectrum in the pure magnetic background (65) for different paths parameterized by $\alpha = 0, 1/4, 1/3, 1/2$. The parameters are set to $Q_1 = Q_2 = \frac{1}{2}Q_s$ and $m/Q_s = 0.1$. We show the absolute value of the spectrum since it is not positive definite over the entire momentum range with this type of Wilson line.

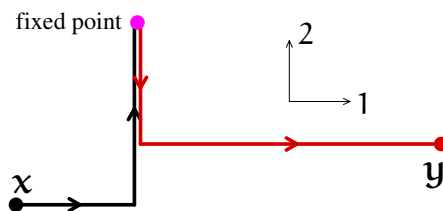
the parameter α that characterizes the shape of the contour. Note that when $\alpha = 1/2$, the path dependent term vanishes and the asymptotic form of the spectrum coincides with that computed with a straight Wilson line, given in eq. (33). In the figure 5, the spectrum (65) is plotted as a function of p_x for several values of α . Since the spectrum depends on α only through $(2\alpha - 1)^2$, it is sufficient to consider $\alpha \in [0, 1/2]$. We can confirm that the p_{\perp}^{-4} tails depend on the path parameter α .

C.2 Paths going through a fixed point

Next, as an explicit example of path that goes through a fix point, we consider a piecewise linear path defined by

$$\gamma : \mathbf{x}_{\perp} \equiv (x^1, x^2) \rightarrow (0, x^2) \rightarrow (0, 0) \rightarrow (0, y^2) \rightarrow \mathbf{y}_{\perp} \equiv (y^1, y^2),$$

as shown here:



In a pure magnetic background, the Wilson line on this path is

$$W_{\gamma}(\mathbf{x}_{\perp}, \mathbf{y}_{\perp}) = e^{-iQ_1\sigma^1 x^1} e^{-iQ_2\sigma^2(x^2-y^2)} e^{iQ_1\sigma^1 y^1}. \quad (67)$$

Its Fourier transform is

$$\widetilde{W}_{\gamma}(\mathbf{k}_{\perp}) = \frac{S_{\perp}}{4} \sum_{\lambda_1, \lambda_2 = \pm} (1 + \lambda_1 \sigma^1) (2\pi)^2 \delta(\mathbf{k}_{\perp} - \lambda_1 \mathbf{Q}_1 - \lambda_2 \mathbf{Q}_2) \quad (68)$$

for $Q_1 \neq 0$, and the quark spectrum reads

$$\frac{dN}{dy_p d^2 \mathbf{p}_{\perp}} = \frac{S_{\perp}}{32\pi^4} \sum_{\epsilon_1, \epsilon_2, \lambda_1, \lambda_2 = \pm} [1 - (1 + \lambda_1 \epsilon_1) G(\mathbf{p}_{\perp}, \lambda_1 \mathbf{Q}_1 + \lambda_2 \mathbf{Q}_2, \epsilon_1 \mathbf{Q}_1, \epsilon_2 \mathbf{Q}_2)]. \quad (69)$$

This spectrum has an unphysical p_{\perp}^{-2} tail at high p_{\perp} as shown in the figure 4.

References

- [1] Edmond Iancu, Andrei Leonidov, and Larry McLerran. The Color glass condensate: An Introduction. In *QCD perspectives on hot and dense matter. Proceedings, NATO Advanced Study Institute, Summer School, Cargese, France, August 6-18, 2001*, pages 73–145, 2002.
- [2] Heribert Weigert. Evolution at small $x(bj)$: The Color glass condensate. *Prog. Part. Nucl. Phys.*, 55:461–565, 2005.
- [3] T. Lappi. Small x physics and RHIC data. *Int. J. Mod. Phys.*, E20(1):1–43, 2011.
- [4] Francois Gelis, Edmond Iancu, Jamal Jalilian-Marian, and Raju Venugopalan. The Color Glass Condensate. *Ann. Rev. Nucl. Part. Sci.*, 60:463–489, 2010.
- [5] F. Gelis. Color Glass Condensate and Glasma. *Int. J. Mod. Phys.*, A28:1330001, 2013.
- [6] Larry D. McLerran and Raju Venugopalan. Computing quark and gluon distribution functions for very large nuclei. *Phys. Rev.*, D49:2233–2241, 1994.
- [7] Larry D. McLerran and Raju Venugopalan. Gluon distribution functions for very large nuclei at small transverse momentum. *Phys. Rev.*, D49:3352–3355, 1994.
- [8] Alex Krasnitz and Raju Venugopalan. Nonperturbative computation of gluon minijet production in nuclear collisions at very high-energies. *Nucl. Phys.*, B557:237, 1999.
- [9] Alex Krasnitz and Raju Venugopalan. The Initial energy density of gluons produced in very high-energy nuclear collisions. *Phys. Rev. Lett.*, 84:4309–4312, 2000.
- [10] T. Lappi. Production of gluons in the classical field model for heavy ion collisions. *Phys. Rev.*, C67:054903, 2003.
- [11] Alex Kovner, Larry D. McLerran, and Heribert Weigert. Gluon production from nonAbelian Weizsacker-Williams fields in nucleus-nucleus collisions. *Phys. Rev.*, D52:6231–6237, 1995.
- [12] Jean-Paul Blaizot and Yacine Mehtar-Tani. The Classical field created in early stages of high energy nucleus-nucleus collisions. *Nucl. Phys.*, A818:97–119, 2009.
- [13] F. Gelis, K. Kajantie, and T. Lappi. Quark-antiquark production from classical fields in heavy ion collisions: 1+1 dimensions. *Phys. Rev.*, C71:024904, 2005.

- [14] F. Gelis, K. Kajantie, and T. Lappi. Chemical thermalization in relativistic heavy ion collisions. *Phys. Rev. Lett.*, 96:032304, 2006.
- [15] Florian Hebenstreit, Juergen Berges, and Daniil Gelfand. Simulating fermion production in 1+1 dimensional QED. *Phys. Rev.*, D87(10):105006, 2013.
- [16] Florian Hebenstreit, Juergen Berges, and Daniil Gelfand. Real-time dynamics of string breaking. *Phys. Rev. Lett.*, 111:201601, 2013.
- [17] Valentin Kasper, Florian Hebenstreit, and Juergen Berges. Fermion production from real-time lattice gauge theory in the classical-statistical regime. *Phys. Rev.*, D90(2):025016, 2014.
- [18] Francois Gelis and Naoto Tanji. Quark production in heavy ion collisions: formalism and boost invariant fermionic light-cone mode functions. *JHEP*, 02:126, 2016.
- [19] Francois Gelis and Naoto Tanji. Schwinger mechanism revisited. *Prog. Part. Nucl. Phys.*, 87:1–49, 2016.
- [20] D. Gelfand, F. Hebenstreit, and J. Berges. Early quark production and approach to chemical equilibrium. *Phys. Rev.*, D93(8):085001, 2016.
- [21] Naoto Tanji and Juergen Berges. Nonequilibrium quark production in the expanding QCD plasma. *Phys. Rev.*, D97(3):034013, 2018.
- [22] F. Gelis and A. Peshier. Probing colored glass via q anti-q photoproduction. *Nucl. Phys.*, A697:879–901, 2002.
- [23] D. Kharzeev and K. Tuchin. Open charm production in heavy ion collisions and the color glass condensate. *Nucl. Phys.*, A735:248–266, 2004.
- [24] Jean Paul Blaizot, Francois Gelis, and Raju Venugopalan. High-energy pA collisions in the color glass condensate approach. 2. Quark production. *Nucl. Phys.*, A743:57–91, 2004.
- [25] Kirill Tuchin. Heavy quark production by a quasiclassical color field in proton nucleus collisions. *Phys. Lett.*, B593:66–74, 2004.
- [26] Naoto Tanji. Nonequilibrium axial charge production in expanding glasma flux tubes. *Phys. Rev.*, D98(1):014025, 2018.
- [27] Francois Gelis and Raju Venugopalan. Large mass q anti-q production from the color glass condensate. *Phys. Rev.*, D69:014019, 2004.

- [28] Hirotugu Fujii, Francois Gelis, and Raju Venugopalan. Quark pair production in high energy pA collisions: General features. *Nucl. Phys.*, A780:146–174, 2006.
- [29] Ninoslav E. Bralic. Exact Computation of Loop Averages in Two-Dimensional Yang-Mills Theory. *Phys. Rev.*, D22:3090, 1980.